

# The *Staphylococcus aureus* SrrAB Two-Component System Promotes Resistance to Nitrosative Stress and Hypoxia

Traci L. Kinkel,<sup>a</sup> Christelle M. Roux,<sup>b</sup> Paul M. Dunman,<sup>b</sup> Ferric C. Fang<sup>a,c</sup>

Department of Laboratory Medicine, University of Washington School of Medicine, Seattle, Washington, USA<sup>a</sup>; Department of Microbiology and Immunology, University of Rochester, Rochester, New York, USA<sup>b</sup>; Department of Microbiology, University of Washington School of Medicine, Seattle, Washington, USA<sup>c</sup>

**ABSTRACT** *Staphylococcus aureus* is both a commensal and a pathogen of the human host. Survival in the host environment requires resistance to host-derived nitric oxide (NO $\cdot$ ). However, *S. aureus* lacks the NO $\cdot$ -sensing transcriptional regulator NsrR that is used by many bacteria to sense and respond to NO $\cdot$ . In this study, we show that *S. aureus* is able to sense and respond to both NO $\cdot$  and hypoxia by means of the SrrAB two-component system (TCS). Analysis of the *S. aureus* transcriptome during nitrosative stress demonstrates the expression of SrrAB-dependent genes required for cytochrome biosynthesis and assembly (*qoxABCD*, *cydAB*, *hemABCX*), anaerobic metabolism (*pflAB*, *adhE*, *nrdDG*), iron-sulfur cluster repair (*scdA*), and NO $\cdot$  detoxification (*hmp*). Targeted mutations in SrrAB-regulated loci show that *hmp* and *qoxABCD* are required for NO $\cdot$  resistance, whereas *nrdDG* is specifically required for anaerobic growth. We also show that SrrAB is required for survival in static biofilms, most likely due to oxygen limitation. Activation by hypoxia, NO $\cdot$ , or a *qoxABCD* quinol oxidase mutation suggests that the SrrAB TCS senses impaired electron flow in the electron transport chain rather than directly interacting with NO $\cdot$  in the manner of NsrR. Nevertheless, like NsrR, SrrAB achieves the physiological goals of selectively expressing *hmp* in the presence of NO $\cdot$  and minimizing the potential for Fenton chemistry. Activation of the SrrAB regulon allows *S. aureus* to maintain energy production and essential biosynthetic processes, repair damage, and detoxify NO $\cdot$  in diverse host environments.

**IMPORTANCE** The Hmp flavohemoglobin is required for nitric oxide resistance and is widely distributed in bacteria. Hmp expression must be tightly regulated, because expression under aerobic conditions in the absence of nitric oxide can exacerbate oxidative stress. In most organisms, *hmp* expression is controlled by the Fe-S cluster-containing repressor NsrR, but this transcriptional regulator is absent in the human pathogen *Staphylococcus aureus*. We show here that *S. aureus* achieves *hmp* regulation in response to nitric oxide and oxygen limitation by placing it under the control of the SrrAB two-component system, which senses reduced electron flow through the respiratory chain. This provides a striking example of convergent evolution, in which the common physiological goals of responding to nitrosative stress while minimizing Fenton chemistry are achieved by distinct regulatory mechanisms.

Received 21 August 2013 Accepted 18 October 2013 Published 12 November 2013

**Citation** Kinkel TL, Roux CM, Dunman PM, Fang FC. 2013. The *Staphylococcus aureus* SrrAB two-component system promotes resistance to nitrosative stress and hypoxia. mBio 4(6):e00696-13. doi:10.1128/mBio.00696-13.

**Editor** Michael Gilmore, Harvard Medical School

**Copyright** © 2013 Kinkel et al. This is an open-access article distributed under the terms of the [Creative Commons Attribution-Noncommercial-ShareAlike 3.0 Unported license](https://creativecommons.org/licenses/by-nc-sa/4.0/), which permits unrestricted noncommercial use, distribution, and reproduction in any medium, provided the original author and source are credited.

Address correspondence to Ferric C. Fang, fcfang@uw.edu.

The ubiquitous human pathogen *Staphylococcus aureus* commonly resides in the nose and on the skin, two sites at which nitric oxide (NO $\cdot$ ) is produced in ample quantities by the host (1, 2). NO $\cdot$  is a versatile molecular mediator with broad-spectrum antimicrobial activity resulting primarily from the targeting of heme and nonheme metal centers, protein thiols, and DNA (3). The ability of *S. aureus* to grow despite the presence of NO $\cdot$  concentrations that are inhibitory for many other bacteria has contributed to its success as a pathogen. The resistance of *S. aureus* to nitrosative stress is in part dependent on the Hmp flavohemoglobin, an enzyme that detoxifies NO $\cdot$  by converting it to nitrate (4). Flavohemoglobin expression must be tightly regulated, as this enzyme can also exacerbate oxidative stress when produced in the absence of NO $\cdot$ , either by shuttling electrons to the flavin pool and promoting Fenton chemistry or by the direct generation of superoxide (5).

In many bacteria, *hmp* flavohemoglobin gene expression is regulated by an Rrf2 family transcriptional repressor known as NsrR (5), which is found in most beta- and gammaproteobacteria as well as in many Firmicutes (6). Nitrosylation of an iron-sulfur cluster in NsrR abrogates the protein's ability to bind DNA, allowing *hmp* expression to respond to very low NO $\cdot$  concentrations (7). Regulation by NsrR ensures that *hmp* is expressed only when NO $\cdot$  is present or when iron concentrations are at very low levels. However, *S. aureus* lacks an NsrR homolog (8). Expression of the *S. aureus hmp* flavohemoglobin gene is regulated in part by the two-component system SrrAB, homologous to ResDE in *Bacillus subtilis*. *B. subtilis* differs from *S. aureus* in possessing both NsrR and ResDE, which regulate *hmp* in concert (9). Both the SrrAB regulatory system and the Hmp enzyme are required for *S. aureus* resistance to NO $\cdot$  and virulence in mice (4). An *srrAB* mutant remains attenuated for virulence in an inducible nitric oxide syn-

these gene (*iNOS*) knockout mouse lacking high-output NO $\cdot$  synthesis, whereas the loss of *iNOS* restores full virulence to an *hmp* mutant. This indicates that the role of SrrAB in staphylococcal virulence extends beyond nitrosative stress resistance and that SrrAB-regulated genes in addition to *hmp* contribute to the pathogenesis of staphylococcal infections.

The present study used bioinformatic and transcriptomic approaches to define the genes controlled by SrrAB in *S. aureus*. The contribution of these genes to nitrosative stress resistance and the mechanism of SrrAB activation were subsequently analyzed. The results reveal that *S. aureus* uses the SrrAB two-component regulatory system to meet common physiological goals met by the transcriptional repressor NsrR in other bacteria.

## RESULTS

**Characterization of the SrrAB regulon during nitrosative stress or hypoxia.** To understand the role of the SrrAB two-component system in the resistance of *S. aureus* to nitrosative stress, a microarray analysis was performed to compare gene expression in wild-type (WT) *S. aureus* COL and an isogenic *srrAB* mutant following treatment with the NO $\cdot$  donor diethylamine NONOate (DEA/NO). The results showed that the SrrAB regulon includes genes involved in maintaining the electron transport chain by supporting cytochrome and quinol-oxidase assembly (*ctaB*, *cydAB*, *qoxABCD*) and heme biosynthesis (*hemACDX*), anaerobic metabolism (*pflAB*, *adhE*, *nrdDG*), and NO $\cdot$  detoxification or the repair of nitrosative damage (*hmp*, *scdA*) (Table 1). In contrast to some previous studies (10, 11), no change in the expression of classic staphylococcal virulence factors was observed under these experimental conditions. The SrrAB regulon identified in our microarray studies more closely resembled the ResDE regulon of *B. subtilis*, which controls genes involved in heme biosynthesis, cytochrome biogenesis, and NO $\cdot$  detoxification (12).

To validate the microarray results, quantitative reverse transcription-PCR (qRT-PCR) analysis of NO $\cdot$ -treated (1 mM DEA/NO) or untreated (DEA alone) wild-type and *srrAB* mutant *S. aureus* COL was performed for selected SrrAB-regulated genes (i.e., *pflA*, *hmp*, *nrdG*, *cydA*, and *scdA*) along with positive and negative controls for NO $\cdot$  induction (*ldh1* and *gyrA*, respectively) (Fig. 1A). Under nitrosative stress, the qRT-PCR measurements corroborated the microarray results, showing higher fold induction following NO $\cdot$  treatment in wild-type cells than in an *srrAB* mutant. Comparison of untreated and NO $\cdot$ -treated cells showed that some NO $\cdot$ -induced genes appear to be exclusively regulated by SrrAB (*nrdG*, *cydA*, *scdA*), while others exhibit both SrrAB-dependent and independent NO $\cdot$ -mediated induction (*pflB*, *hmp*). The *ldh1* locus, previously shown to be regulated by the transcriptional repressor Rex, was induced by NO $\cdot$  and uninfluenced by SrrAB. Expression of the housekeeping gene *gyrA* was not altered by nitrosative stress in either wild-type or *srrAB* mutant cells. Additionally, the SrrAB regulon was verified across multiple *S. aureus* strains, including UAMS-1, a biofilm-forming strain (13), and Newman, a virulent clinical isolate (4, 14). The pattern of SrrAB-dependent gene regulation was highly similar across these varied *S. aureus* strains (see Table S1 in the supplemental material).

Previous studies have reported that the SrrAB two-component system is necessary for growth under oxygen-limited conditions (10, 15). We observed that SrrAB-dependent genes expressed during nitrosative stress are also induced during hypoxia in an SrrAB-

TABLE 1 Microarray analysis of gene expression in wild-type and *srrAB* mutant *S. aureus* COL during nitrosative stress<sup>a</sup>

Locus	Description	Gene Name	WT/ <i>srrAB</i>
SA0204	formate acetyltransferase	<i>pflB</i>	9.287
SA0205	pyruvate formate-lyase-activating enzyme	<i>pflA</i>	9.503
SA0660	alcohol dehydrogenase, zinc-containing	<i>adhE</i>	2.364
SA2635	anaerobic ribonucleoside-triphosphate reductase	<i>nrdD</i>	29.800
SA2634	anaerobic ribonucleoside-triphosphate reductase	<i>nrdG</i>	29.767
SA1068	quinol oxidase, subunit III	<i>qoxC</i>	2.317
SA1069	quinol oxidase, subunit I	<i>qoxA</i>	2.257
SA1070	quinol oxidase, subunit II	<i>qoxB</i>	2.331
SA1094	cytochrome d ubiquinol oxidase, subunit I	<i>cydA</i>	12.671
SA1095	cytochrome d ubiquinol oxidase, subunit II	<i>cydB</i>	12.038
SA1125	conserved cytochrome <i>caa3</i> oxidase	<i>ctaB</i>	3.034
SA1126	conserved hypothetical protein		2.812
SA1716	uroporphyrinogen-III synthase	<i>hemD</i>	2.559
SA1717	porphobilinogen deaminase	<i>hemC</i>	2.645
SA1718	hemX protein	<i>hemX</i>	2.864
SA1719	glutamyl-tRNA reductase	<i>hemA</i>	2.178
SA0220	flavo-hemoprotein, putative	<i>hmp</i>	4.984
SA0244	ScdA protein	<i>scdA</i>	6.329
SA0089	antigen, 67 kDa	SA0089	8.345
SA0217	ABC transporter, substrate-binding protein	SA0217	3.427
SA0218	conserved hypothetical protein	SA0218	7.478
SA0219	hypothetical protein	SA0219	8.902
SA2563	ATP-dependent Clp protease, putative	<i>clpL</i>	2.390
SA0095	Immunoglobulin G binding protein A	<i>spa</i>	-1.343
SA0222	Lactate/malate dehydrogenase	<i>ldh1</i>	1.173
SA1842	Accessory gene regulator B	<i>agrB</i>	-1.534
SA2689	intercellular adhesion protein	<i>icaA</i>	-1.174
SA0161	conserved hypothetical protein	SA0161	-2.422
SA1534	staphylococcal respiratory response protein SrrB	<i>srrB</i>	-4.239
SA1783	acetyl-CoA synthetase	<i>acs</i>	-2.296
SA1816	proline dehydrogenase	<i>putA</i>	-2.681
SA2146	PTS system, mannitol-specific IIBC components	SA2146	-2.180
SA2393	respiratory nitrate reductase, delta subunit	<i>narJ</i>	-2.238
SA2394	respiratory nitrate reductase, beta subunit	<i>narH</i>	-2.231
SA2395	respiratory nitrate reductase, alpha subunit	<i>narG</i>	-2.319
SA2463	triacylglycerol lipase precursor	<i>lip</i>	-2.229
SA2516	gluconate operon transcriptional repressor	<i>gntR</i>	-2.090
SA2554	LrgA family protein	<i>cidA</i>	-3.057
SA2569	delta-1-pyrroline-5-carboxylate dehydrogenase	SA2569	-2.089

<sup>a</sup>Bacteria were grown in PN medium treated with 1 mM DEA/NO. Data are presented as the ratio for WT COL/*srrAB*. Colors indicate functional group: pink, anaerobic metabolism; green, cytochrome biosynthesis and assembly; yellow, NO $\cdot$  detoxification and repair; white, hypothetical genes; orange, neutral genes; and blue, negatively regulated genes.

dependent fashion (Fig. 1B), suggesting a common mechanism for SrrAB induction under nitrosative stress and hypoxic conditions.

**Importance of the SrrAB regulon for NO $\cdot$  resistance and anaerobic growth.** Our previous observations have shown that *srrAB* mutant *S. aureus* is more sensitive to NO $\cdot$  than an *hmp* mutant, indicating that additional SrrAB-dependent genes contribute to nitrosative stress resistance (4). To investigate further, mutations were constructed in several SrrAB-regulated genes belonging to different functional groups. These included mutations in two terminal oxidases of the *S. aureus* electron transport chain: *cydAB*, encoding the *bd*-type cytochrome, and *qoxABCD*, encoding the *aa*<sub>3</sub>-type quinol oxidase. In addition, mutations were constructed in *nrdDG*, which encodes a class III ribonucleotide reductase that functions under anaerobic conditions (16), and in *scdA*, encoding a di-iron-containing protein previously implicated in

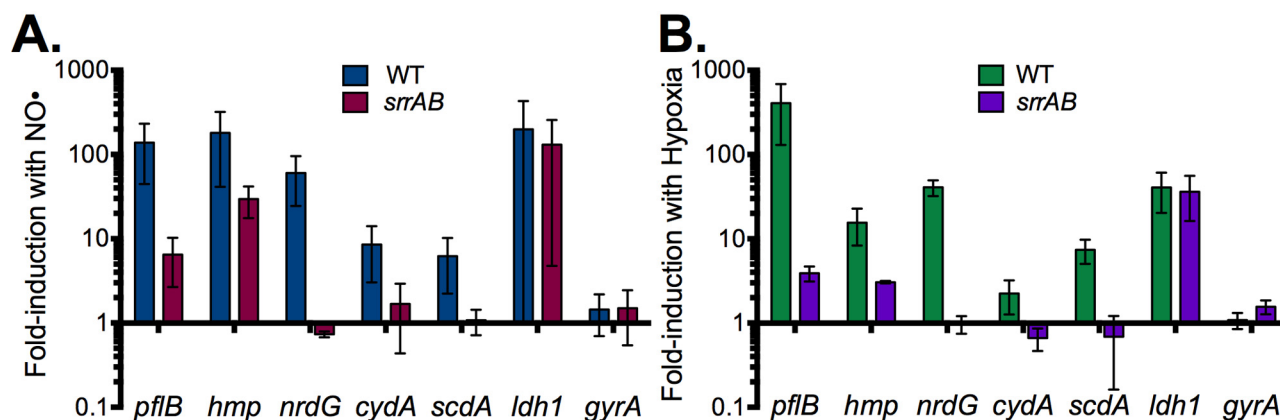


**FIG 1** Expression of SrrAB-regulated genes during nitrosative stress and hypoxia. (A) Wild-type *S. aureus* COL or isogenic *srrAB* mutant strains were grown in PN medium with 1 mM DEA/NO or the DEA parent compound. (B) Wild-type *S. aureus* COL or isogenic *srrAB* mutant strains were grown in TSB medium under aerobic or anaerobic conditions. Data are shown as the log-fold change between the treated (NO· or anaerobic) and untreated (DEA or aerobic) samples normalized to *rpoD* and are the averages from 3 independent experiments; error bars = standard deviation (SD).

the repair of NO--damaged Fe-S clusters (17). An *scdA hmp* double mutant was also constructed to assess the *scdA* phenotype in the absence of the NO--detoxifying activity of Hmp.

The contribution of the SrrAB-regulated genes in resistance to NO· was tested by growth in a Bioscreen C apparatus with (solid lines) or without (dashed lines) the addition of NO· donor compounds NOC-12 (5 mM, half-life [ $t_{1/2}$ ] of 100 min) and DEA/NO (1 mM,  $t_{1/2}$  of 2 min) (Fig. 2A). As before, growth of both *srrAB* and *hmp* mutant strains was found to be significantly impaired during nitrosative stress ( $P < 0.0005$  and  $P < 0.005$ , respectively). Mutations in other individual SrrAB-regulated genes conferred various degrees of enhanced susceptibility to NO·. An *nrdDG* mutant showed only minimal and nonsignificant impairment in NO·-resistance under the aerobic conditions tested, while *cydAB* or *scdA* mutants exhibited slightly more pronounced phenotypes that also failed to achieve statistical significance. A *qoxABCD* mutant was found to be significantly more sensitive to nitrosative stress compared to the wild type ( $P < 0.05$ ), although this mutant also appeared to exhibit a modest growth defect under aerobic conditions in the absence of NO·. Collectively, these results suggest that the NO·-susceptibility phenotype of an *srrAB* mutant represents additive effects from multiple SrrAB-regulated loci, particularly *hmp* and *qoxABCD*. To investigate this possibility, double mutants were constructed containing *hmp* and either *cydAB* or *qoxABCD* mutations. The NO·-resistance of a *cydAB hmp* double mutant was only slightly greater than that of the *hmp* mutant alone (Fig. 2B). However, growth of a *qoxABCD hmp* mutant after NO· treatment was comparable to that of an *srrAB* mutant ( $P < 0.0001$ ), indicating that collectively these two loci account for most of the contribution of SrrAB to nitrosative stress resistance.

Previous studies have also implicated SrrAB in growth under anaerobic conditions (10, 15). To analyze the contribution of individual SrrAB-regulated genes to anaerobic growth, the growth of wild-type and mutant strains was measured with aeration (shaking), under standing (static) conditions, and in an anaerobic jar. Our results confirm previous studies showing that SrrAB is required for maximal growth under anaerobic conditions ( $P < 0.0001$ ) (Fig. 2C). Of the SrrAB-regulated genes tested, only *nrdDG* had a measurable impact on anaerobic growth ( $P < 0.0001$ ). The *srrAB* and *qoxABCD* mutant strains were unable to

attain maximal final cell density under aerobic conditions ( $P < 0.005$  and  $P < 0.0005$ , respectively) but showed no significant difference under either static or anaerobic conditions. Thus, the SrrAB two-component system is activated during nitrosative stress or hypoxia and regulates genes that are important for survival and growth under these conditions.

**Importance of SrrAB for NO· detoxification.** One of the principal biological effects of NO· is the rapid and reversible inhibition of respiration due to reversible binding of NO· to cytochrome heme centers (18). Respiration is restored once NO· is detoxified, and *hmp* expression is a major determinant of the duration of respiratory inhibition following bolus administration of NO·. We have previously shown that the inhibition of respiration following treatment of *srrAB* mutant *S. aureus* with an NO· donor is intermediate between that of wild-type and *hmp* mutant *S. aureus*, presumably because *hmp* expression is not completely SrrAB-dependent (Fig. 1) (4). In the present study, respiration was monitored following the treatment of *cydAB* or *qoxABCD* single mutant strains along with double *hmp* mutant strains, and the results were compared with those of wild-type, *srrAB* mutant, and *hmp* mutant strains. Both oxygen and NO· consumption were recorded, but for clarity only NO· consumption is shown in Fig. 3A (representative respiratory inhibition curves for each strain are provided in Fig. S2 in the supplemental material). Wild-type, *srrAB* mutant, and *hmp* mutant strains yielded expected results based on prior studies, and a *cydAB* mutant exhibited an NO·-consumption rate similar to that of the wild type. This suggests that the *bd*-type cytochrome is not favored under typical aerobic conditions (19). Unexpectedly, the *qoxABCD* mutant strain exhibited significantly more rapid NO· consumption (Fig. 3A) and a correspondingly briefer period of respiratory inhibition than the wild type (see Fig. S2E in the supplemental material). The *cydAB hmp* and *qoxABCD hmp* double mutants were unable to resume respiration after the addition of NO·, phenocopying the single *hmp* mutant (data not shown).

We hypothesized that the increased NO·-resistance of a *qoxABCD* mutant might result from increased *hmp* expression. This was confirmed by measurement of *hmp* expression in wild-type and *qoxABCD* mutant cells by qRT-PCR during late-logarithmic-phase growth (Fig. 3B). Under conditions in which respiration

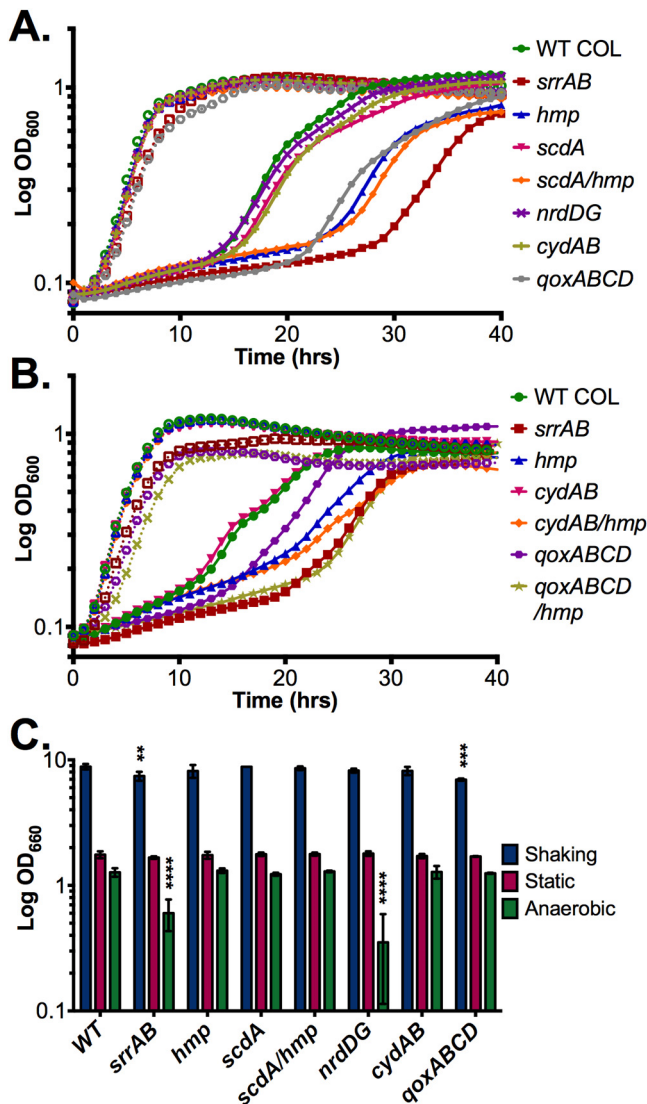


**FIG 2** Effects of SrrAB and SrrAB-regulated genes on growth during nitrosative stress and hypoxia. Wild-type *S. aureus* COL or isogenic *srrAB* (\*\*), *hmp* (\*\*), *scdA*, *scdA hmp* (\*), *nrdDG*, *cydAB*, and *qoxABCD* (\*) mutants (A) and wild-type *S. aureus* COL or isogenic *srrAB* (\*), *hmp* (\*\*\*\*), *cydAB*, *cydAB hmp* (\*\*\*\*), *qoxABCD* (\*\*), and *qoxABCD hmp* (\*\*\*\*) mutants (B) were grown in PN medium with (solid lines) or without (dotted lines) the addition of 5 mM NOC-12 and 1 mM DEA/NO. Data shown are the averages from 4 independent experiments (2 experiments for the *scdA hmp* mutant). Statistical significance was determined by Student's *t* test comparing  $\Delta t$  (NO $_2^-$  treated minus untreated) to reach an OD $_{660}$  of 0.3 compared to that of the wild type. (C) Cells were grown under shaking, static, or anaerobic conditions. A 24-h OD $_{660}$  reading was recorded for each sample from at least three independent cultures; error bars = SD. Significance was determined by Student's *t* test comparing each mutant to the wild type (\*,  $P < 0.05$ ; \*\*,  $P < 0.005$ ; \*\*\*,  $P < 0.0005$ ; and \*\*\*\*,  $P < 0.0001$ ).

was induced by the addition of glucose or following treatment with 5  $\mu$ M Proli-NO, expression of *hmp* was 2- and 3.5-fold higher, respectively, in a *qoxABCD* mutant than in the wild type (Fig. 3B). NAD $^+$ /NADH ratios for wild-type and *qoxABCD* mutant cells under these assay conditions were unchanged (data not shown). These results suggest that the increased NO $_2^-$  consumption and resistance observed in a *qoxABCD* mutant strain result from increased *hmp* expression.

**Importance of SrrAB for biofilm formation.** The ability to form and sustain biofilms is considered to be an important virulence-associated phenotype of *S. aureus* that is likely to be of particular relevance to device-associated infections. *S. aureus* is also capable of forming biofilms in bone and other tissues. Biofilms may be difficult to treat with antibiotics because of limited penetration and phenotypic resistance of organisms in the biofilm state. As the ability to sense oxygen and grow in oxygen-limited conditions is necessary for biofilm formation, we determined whether the SrrAB two-component system affects *S. aureus* biofilm formation *in vitro*. Because *S. aureus* strain COL does not form biofilms, *srrAB* and *hmp* mutations were constructed in the biofilm-forming strain UAMS-1 (13, 20). The UAMS-1 strains were tested and shown to have similar SrrAB-dependent gene regulation and NO $_2^-$  resistance phenotypes (see Table S1 and Fig. S1A in the supplemental material). UAMS-1 forms primarily proteinaceous biofilms, in contrast to the polysaccharide intercellular adhesin (PIA) capsule-associated biofilms of other *S. aureus* strains (21). Biofilm formation was initially evaluated by a 1- to 3-day static biofilm method in human plasma-coated 96-well plates and quantified with crystal violet staining. Using this biofilm method, we identified that the *srrAB* mutant has reduced capacity to form biofilms over time compared to the WT. The *sarA* mutant strain, previously reported to be defective at biofilm formation, was used as a negative control (22). Over a 3-day period, a gradual decrease in biofilm formation by the *srrAB* mutant in comparison with the WT was observed: 83.3%, 51.9%, and 35.6% on days 1, 2, and 3, respectively (Fig. 4A). The *hmp* mutant did not show any difference in biofilm levels compared to WT UAMS-1.

After observing that an *srrAB* mutant exhibited decreased biofilm formation over time compared to that of the wild-type *S. aureus* under static aeration conditions (Fig. 2B), we hypothesized that SrrAB may be more important during long-term persistence of biofilms as cell density increases and oxygen and nutrients become limiting. We therefore utilized an alternative static biofilm method in which biofilms are grown on a glass coverslip over a 5-day period, to allow visualization via confocal microscopy and staining with BacLight (Invitrogen) (23). Culture medium was changed daily, and biofilms were washed with phosphate-buffered saline (PBS) to remove nonadherent cells. Each day, biofilms were collected from WT *S. aureus* UAMS-1 and isogenic *srrAB* and *hmp* mutant strains for the duration of the experiment. Biofilms were stained with BacLight (Invitrogen), which labels viable cells with SYTO-9 and nonviable cells with propidium iodide (PI), and visualized using confocal laser scanning microscopy (LSM). All three strains were able to initiate biofilm formation with similar thickness (~20 to 25  $\mu$ M) observed on day 1 (data not shown) and day 2 (Fig. 4B). By day 4, the biofilms formed by the *srrAB* mutant strain began to deteriorate and were found to contain significantly more dead cells than either the wild-type or *hmp* mutant biofilms. To quantify dead cells within the biofilm, profile images from at least 3 different regions were examined on 2 different slides per day for each strain. The *srrAB* mutant biofilms contained ~5% more dead cells than wild-type biofilms on days 1 and 2 but contained ~10% more dead cells on days 3 to 5 (42.5% dead cells in *srrAB* mutant biofilms versus 32.5% in the wild type) (Fig. 4C). The increase in dead cells corresponded to the loss of structural integrity in the *srrAB* mutant biofilms and suggests that the SrrAB two-component regulatory system is important for long-term biofilm stability and survival. The *hmp* mutant displayed higher

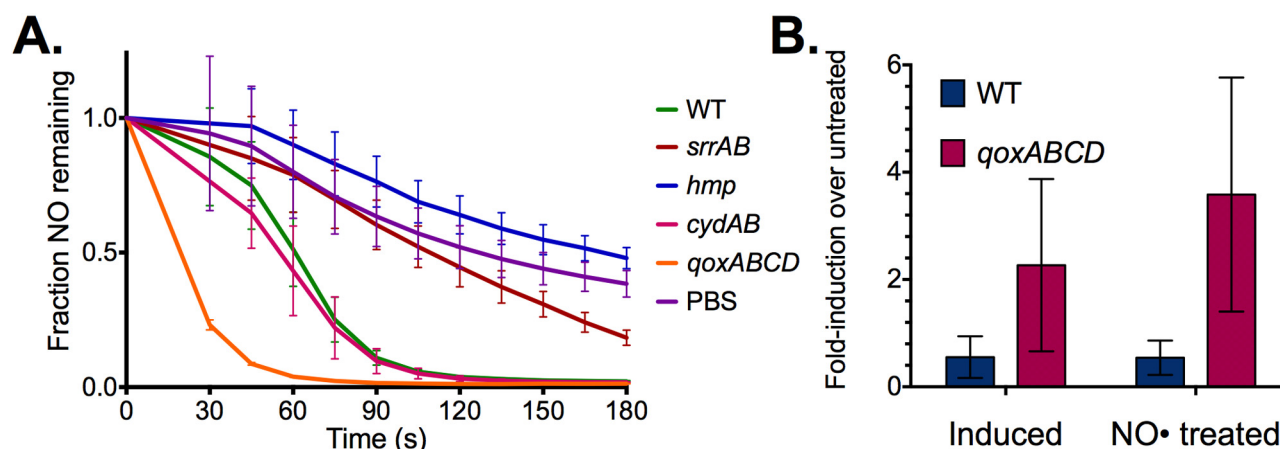


**FIG 3** NO• consumption by wild-type or mutant *S. aureus*. (A) NO• consumption was monitored after the addition of 5  $\mu\text{M}$  Proli/NO to wild-type *S. aureus* COL or isogenic *srrAB*, *hmp*, *cydAB*, and *qoxABCD* mutants and compared to a PBS control. The mean fraction of remaining NO• from 3 independent experiments is shown; error bars = SD. Statistical analysis was performed using a matched two-way ANOVA with Bonferroni post-test analysis. Significant differences in comparison to the wild type were found for the *srrAB* mutant, *hmp* mutant, *qoxABCD* mutant, and PBS control ( $P < 0.0001$ ). Differences in NO• consumption by the *cydAB* mutant were not significant. (B) Quantitative RT-PCR was performed on wild-type *S. aureus* COL or an isogenic *qoxABCD* mutant from untreated, glucose-treated (respiration-induced), and NO•-treated samples. Data shown are from 3 independent experiments and expressed as fold-induction of *hmp* normalized to *rpoD* from untreated cells.

levels of dead cells on day 1 ( $P < 0.05$ ), but this number did not increase over time and was not significantly different from the WT on subsequent days.

## DISCUSSION

Survival of *Staphylococcus aureus* within the human host depends on the microbe's ability to sense and respond to diverse environments. Nitrosative stress resulting from the enzymatic or nonenzymatic synthesis of NO• is one of the most important environmental conditions to which staphylococci must adapt. The activation of SrrAB signaling by either NO• or hypoxia suggested that these signals converge upon a common regulatory pathway. Our observations are consistent with a model (Fig. 5) in which reduced menaquinone triggers the SrrB-dependent phosphorylation of SrrA, which in turn activates genes required for anaerobic metabolism, cytochrome and heme biosynthesis, and NO• detoxification. In addition to promoting the expression of Hmp, the SrrAB two-component system promotes NO• resistance by increasing the expression of inhibited metabolic pathways (PflBA, HemACDX, QoxABCD, CydAB, CtaB), upregulating alternative pathways (e.g., NrdDG) to bypass targets of NO• inhibition, and activating repair systems (ScdA). These functions appear to have an additive effect in NO• resistance (Fig. 2A). In contrast to earlier studies (10, 11), we did not find evidence that classical virulence genes (e.g., *spa*, RNIII gene, *ica*) are regulated by SrrAB under our experimental conditions. Hmp expression remains inducible by NO• in an *srrAB* mutant strain (Fig. 1A), and the mechanism responsible for SrrAB-independent activation of *hmp* is presently unknown.

The branched electron transport chain of *S. aureus* can terminate in an  $aa_3$ -type cytochrome encoded by *qoxABCD* or an alternative  $bd$ -type cytochrome encoded by *cydAB* (19, 24). While most bacteria utilize multiple quinone variants as electron carriers, *S. aureus* uses menaquinone exclusively. The inhibition of terminal oxidases by NO• or by oxygen limitation limits flow through the electron transport chain, thereby triggering SrrAB

activation. A *qoxABCD* mutation mimics this process (Fig. 3B and 5). By placing *hmp* under the control of SrrAB in response to flux through the electron transport chain, *S. aureus* achieves the central aim of limiting Hmp flavohemoglobin expression unless NO• is present and/or oxygen levels are low. We observed a *qoxABCD* mutation abrogating cytochrome  $aa_3$  to have a greater effect on NO• sensitivity than a *cydAB* mutation in *S. aureus*. This suggests that QoxABCD is the preferred terminal oxidase in *S. aureus* during nitrosative stress. A *qoxABCD* mutant actually exhibited more rapid NO• detoxification due to compensatory SrrAB activation and increased *hmp* expression. A recent study has suggested that the *S. aureus* *cydAB* genes may have been misannotated and might not actually encode a  $bd$ -type cytochrome (25). Additionally, heme-spectral analysis of the *S. aureus* cytochromes indicates the presence of a  $bo$ -type and a  $ba_3$ -type cytochrome (26). The present study shows that an *S. aureus* *cydAB* mutant is not more susceptible to NO•, in contrast to *Escherichia coli* (27), lending further support to the idea that *cydAB* may not encode a  $bd$ -type cytochrome.

A *menD* mutation, which abrogates menaquinone biosynthesis, has been previously shown to result in the loss of expression of SrrAB-dependent genes and the upregulation of *srrAB* itself (28). This is consistent with the direct sensing of reduced menaquinone by SrrB, as observed for ArcB in enteric bacteria (29). By monitoring electron transport, SrrAB complements the regulatory function of the repressor Rex, which is responsive to NAD<sup>+</sup>/NADH balance, in maintaining redox homeostasis (30). Both SrrAB and Rex respond to changes induced during nitrosative stress, leading to the upregulation of diverse regulons necessary for survival under these conditions. Interestingly, Rex appears to bind upstream of *srrAB*, and SrrA protein levels are increased in a Rex mutant; however, transcript levels do not appear to be altered significantly, suggesting a more complex regulatory mechanism (30).

The induction of SrrAB by hypoxia and the reduced survival of an *srrAB* mutant during anaerobic growth (Fig. 2C) suggested a

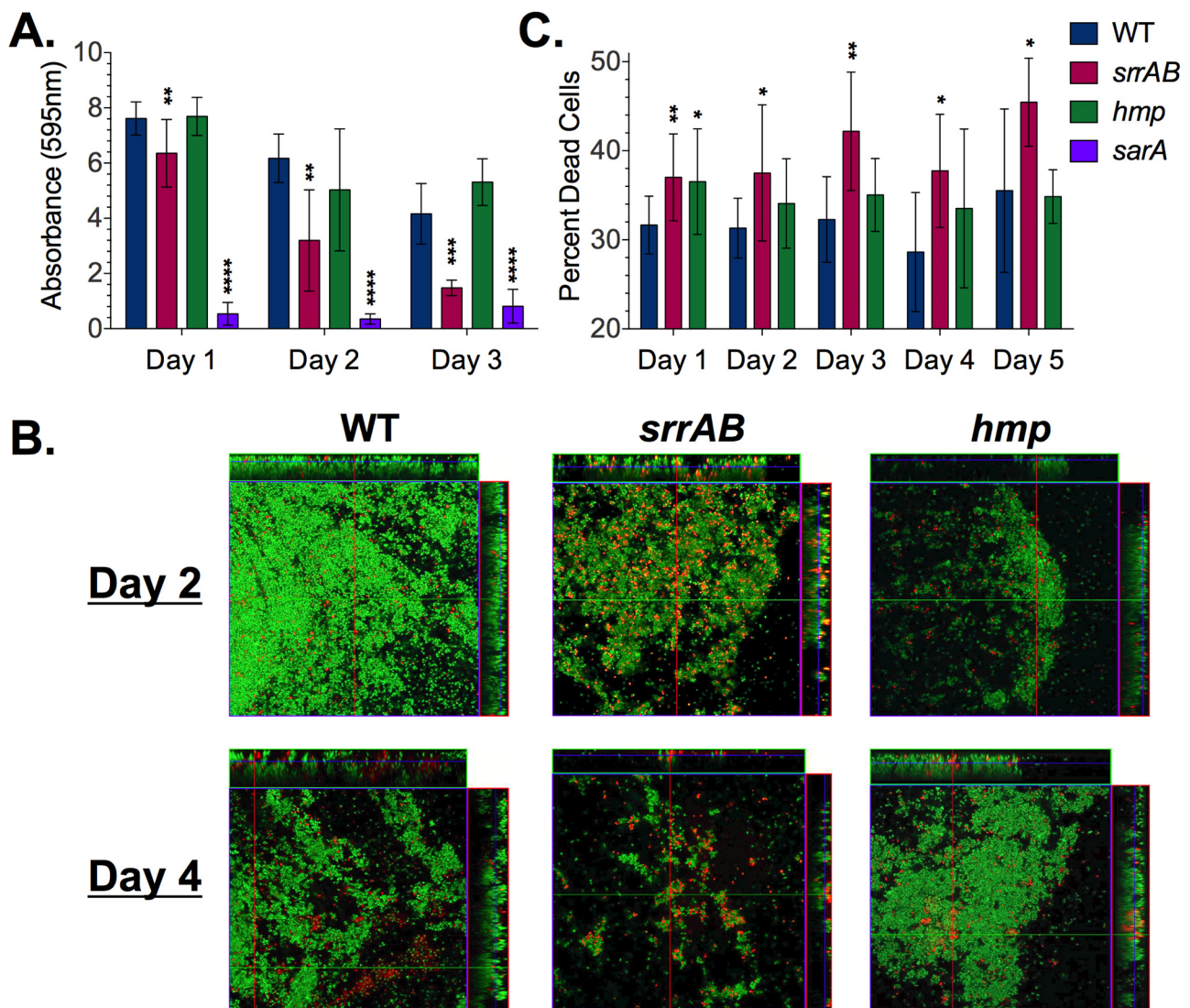


**FIG 4** Biofilm formation by wild-type and mutant *S. aureus*. Wild-type *S. aureus* UAMS-1 or isogenic *srrAB*, *hmp*, and *sarA* mutants were grown in TSBGN medium for 3 to 5 days in either 24-well or 6-well tissue culture plates with sterile coverslips pretreated with 20% human plasma. (A) Biofilms were quantified with crystal violet staining, and the absorbance at 595 nm was read for 3-fold dilutions of the crystal violet elution. Shown is the result from 3 independent experiments with at least 6 wells per strain; error bars = SD. (B) A minimum of 3 different coverslips were analyzed for each strain on each day. Biofilms were stained with SYTO-9 and propidium iodide and imaged with a Zeiss 510-Meta confocal microscope. The orthogonal images are representative of biofilms from days 2 and 4. (C) Split-color biofilm profile images were analyzed using ImageJ for integrated density to determine the relative percentage of live and dead cells in each image. At least 7 profile images were analyzed for each strain on each day; error bars = SD. Significance for panels A and C was calculated using Student's *t* test comparing means to the WT for each day (\*,  $P < 0.05$ ; \*\*,  $P < 0.01$ ; \*\*\*,  $P < 0.001$ ; and \*\*\*\*,  $P < 0.0001$ ).

possible role for SrrAB in biofilms, an oxygen-limited growth condition. Indeed, we found that *srrAB* mutant *S. aureus* exhibits grossly deficient biofilm formation with increased levels of cell death (Fig. 4A and C), a finding corroborated by the results of an earlier mutant screen that identified *srrA* as essential for PIA-independent biofilm formation (31). The defective biofilm phenotype did not appear to be related to NO $\cdot$ , as an isogenic *hmp* mutant was unimpaired in overall biofilm formation.

In summary, although *S. aureus* lacks the NO $\cdot$ -sensing transcription factor NsrR, it achieves NO $\cdot$ -responsive expression of the NO $\cdot$ -detoxifying Hmp flavohemoglobin by means of the SrrAB two-component system that senses flux through the electron transport chain. The SrrAB regulon coordinately controls

metabolic, detoxification, and repair systems that play an essential role in staphylococcal adaptation to hypoxic and nitrosative stress environments encountered within the infected host. This underscores the intimate relationship between bacterial metabolism and pathogenesis.

#### MATERIALS AND METHODS

**RNA isolation and microarray studies.** Both WT COL and an isogenic *srrAB* mutant (4) were grown in PN medium (32) to an optical density at 660 nm ( $OD_{660}$ ) of 0.5, and cells were split into treated or untreated samples. Cells in the treated group were incubated with 1.1 mM of the NO $\cdot$  donor compound DEA/NO (half-life of 2 min) for 20 min, while those in the untreated group were incubated with the parent nucleophile

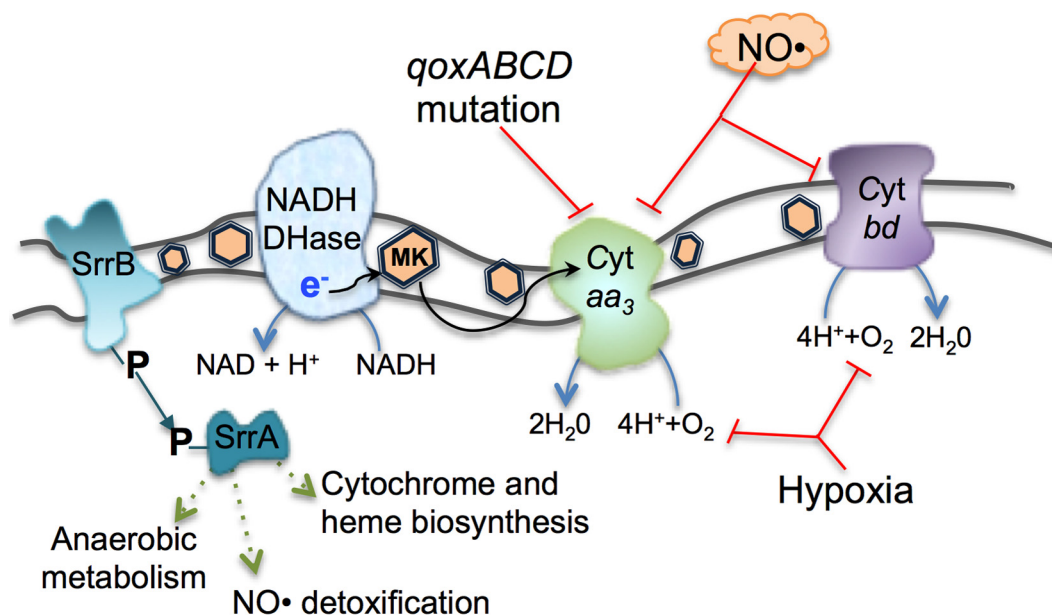


**FIG 5** Model of SrrAB activation by nitrosative stress or hypoxia. Nitric oxide (NO $\cdot$ ), a quinol oxidase (*qoxABCD*) mutation, or oxygen limitation impairs the flow of electrons through the electron transport chain. Sensing of reduced menaquinone by SrrB results in phosphorylation of SrrA and subsequent activation of downstream genes.

DEA for the same amount of time. After incubation, cells were immediately mixed 1:1 with an ice-cold 1:1 mixture of 100% ethanol and acetone and placed at  $-80^{\circ}\text{C}$  until RNA was isolated. RNA was isolated from approximately  $5 \times 10^9$  CFU and lysed by bead beating for two 40-s pulses separated by 5 min of incubation on ice, followed by pelleting of cell debris and beads. Supernatant was removed from the beads and used for RNA purification by the Qiagen RNeasy Midi protocol. RNA was eluted in diethyl pyrocarbonate (DEPC)-treated  $\text{H}_2\text{O}$  and quantified with a Shimadzu spectrophotometer. RNA was tested for induction of *hmp* expression after NO $\cdot$  treatment to verify the inducing conditions prior to microarray analysis. Microarray studies were performed as previously described (4, 33) using at least two biological replicates of the NO $\cdot$ -treated WT and *srrAB* mutant samples.

**qRT-PCR assay of gene expression.** To verify the microarray results, treated and untreated RNA samples from the microarray studies were analyzed by quantitative real-time RT-PCR. The Qiagen 1-step SYBR mix was used, preceded by an additional cDNA conversion step. Primer sets for the analyzed genes are listed in Table S2 in the supplemental material. qRT-PCR analysis was performed using a Rotor-Gene (Qiagen, Valencia, CA). Data were analyzed by comparing relative steady-state mRNA concentration of the gene of interest to that of the housekeeping *spoD* gene, and fold induction during treatment with NO $\cdot$  was calculated.

For measurement of gene expression under hypoxic conditions, WT *S. aureus* COL and an isogenic *srrAB* mutant were grown aerobically with shaking in tryptic soy broth (TSB) medium to an OD $_{660}$  of 0.5. Cells were then transferred either to a 15-ml conical tube, which was filled to the top with the cap fully tightened, or to a 5-ml glass tube and incubated with shaking for 30 min before mixing with an ice-cold (1:1) EtOH acetone mixture. All other RNA was prepared using the Qiagen mini-prep system with lysis via bead beating and analyzed via a 2-step RT-PCR process. RNA was converted to cDNA (QuantiTect, Qiagen) before cDNA was diluted 1:25 for use with the Qiagen FAST-SYBR kit. Data were analyzed as described above.

**Strain construction.** Mutations in *cydAB*, *nrdDG*, *scdA*, *qoxABCD*, and *srrB* were constructed using the temperature-sensitive plasmid pBT2 (34), with primer pairs listed in Table S2 in the supplemental material and the  $\Omega\text{Km}$  cassette from pUC-4  $\Omega\text{Km}2$  (gift from Kevin McIver). All basic

cloning was performed in *E. coli* DH10b, using ampicillin at  $100 \mu\text{g ml}^{-1}$ . The *cydAB*, *nrdDG*, *scdA*, and *srrB* fragments were amplified using L and R primers containing BamHI and XhoI restriction sites, and the *qoxABCD* fragment was amplified without any restriction sites (listed in Table S2), before the digested PCR product was cloned into vector pJK392 or a modified version (pTK392) in which the NdeI site was filled in and religated. The resulting constructs were digested using the following conditions: *cydAB*, EcoRI digested and filled in; *nrdDG*, HpaI-digested, which deletes an  $\sim 300$ -bp region; *scdA* and *qoxABCD*, NdeI digested and filled in; and *srrB*, HindIII digested and filled in. All were ligated with the SmaI-digested  $\Omega\text{Km}$  fragment from pUC-4  $\Omega\text{Km}2$ . Each fragment containing *cydAB*, *nrdDG*, *scdA*, *qoxABCD*, or *srrB* with  $\Omega\text{Km}$  was removed from pJK392 or pTK392 with KpnI and XbaI, and ends were filled in and then blunt ligated into the EcoRV site of the pBT2 shuttle vector. These plasmids, designated pTK1, pTK2, pTK3, pTK4, or pTK5, respectively, were purified from DH10b, transformed into *S. aureus* strain RN4220, and maintained using kanamycin at  $100 \mu\text{g ml}^{-1}$  and chloramphenicol at  $10 \mu\text{g ml}^{-1}$ . From RN4220, plasmids were transduced into *S. aureus* strain COL (8) using bacteriophage phi-11 (35). Recombination events occurred following passage at the permissive temperature of  $30^{\circ}\text{C}$  and switching to  $43^{\circ}\text{C}$ , followed by serial passage at  $30^{\circ}\text{C}$  without selection to allow for double recombination. A cycloserine enrichment process was used to select Cm $^s$  recombinants. Mutants were verified by PCR amplification of the flanking region and an internal primer for the  $\Omega\text{Km}$ -cassette (see Table S2).

Double *hmp* mutants and mutations in UAMS-1 (*srrAB* and *hmp*) were constructed using phage transduction (phi-11) from RN4220 containing pTR43 (*srrAB*) and pTR40 (*hmp*). Similar passaging at  $30^{\circ}\text{C}$  and  $43^{\circ}\text{C}$  and cycloserine-enrichment protocols were followed as described above. When indicated, erythromycin was added at  $5 \mu\text{g ml}^{-1}$ .

**Measurement of NO $\cdot$  susceptibility.** Cells were grown overnight in TSB and then diluted to an OD $_{660}$  of 1.0 in PN medium. A further 1:30 dilution was made for each strain before being added to the Bioscreen C plate (Growth Curves United States, Piscataway, NJ) for incubation with maximal shaking at  $37^{\circ}\text{C}$  for 40 h with or without the addition of the NO $\cdot$ -donating compounds DEA/NO (1 mM) and NOC-12 (5 mM).

**Measurement of hypoxic growth.** Colonies of each strain were isolated from tryptic soy agar (TSA) plates and inoculated into 9 ml of TSB. Subcultures were split into three equivalent 3-ml samples in 13- by 100-mm glass tubes. One tube was placed on a shaker (~250 rpm), one was incubated statically on a shelf, and one was placed inside an anaerobic jar with a BD BBL GasPak Plus envelope at 37°C for 24 h. A 24-h OD<sub>660</sub> reading was taken using a Bio-Rad SmartSpec 3000.

**Measurement of respiration inhibition by NO·.** To monitor the inhibition of respiration by NO·, both NO· and O<sub>2</sub> levels were monitored using specific electrodes. To measure [NO·], an ISO-NO MarkII NO-meter (World Precision Instruments, Sarasota, FL) with an ISO-NOP NO· probe was used. To measure [O<sub>2</sub>], an MI-730 oxygen probe with the O<sub>2</sub>-ADPT oxygen adapter (Microelectrodes Inc., Bedford, NH) was used. The output from both probes was recorded using LABCHART software (ADI Instruments, Colorado Springs, CO). Cells were grown in TSB to an OD<sub>660</sub> of 1.0, upon which they were spun down in 25-ml aliquots, rinsed with PBS, and then repelleted. Cultures were kept on ice until assayed. For assays, cells were resuspended in PBS that had been bubbled with O<sub>2</sub> for 30 min at 37°C. Upon resuspension, cells were immediately transferred to a beaker, where the probes were set to begin recording. One minute after transferring the cells, 20% glucose was added to a final concentration of 0.1% to stimulate respiration. When approximately 75% O<sub>2</sub> remained, a 10 μM bolus of NO· was added (Prolin-NO; half-life of 1.3 s). Recordings were carried out until all oxygen had been consumed or until 12 min after the addition of glucose.

Data were analyzed by determining the maximal point of NO· in the PBS control and calculating the fraction of NO· remaining for each strain tested. This experiment was repeated 3 independent times for each strain.

**Biofilm growth and analysis.** Static biofilms were grown using conditions described previously, with WT *S. aureus* strain UAMS-1 and isogenic *sarA*, *srrAB*, and *hmp* mutants (13, 22). Briefly, for the crystal violet biofilm assays, 24-well tissue culture plates were used, and for confocal microscopy studies, sterile coverslips were placed into 6-well tissue culture dishes. The tissue culture dishes were precoated with 20% human plasma diluted in 0.1 M carbonate buffer (pH 9.6) for 24 h at 4°C. *S. aureus* UAMS-1 and isogenic mutant strains were grown overnight in TSB supplemented with 0.5% glucose and 3% sodium chloride. The overnight cultures were diluted 1:200 into either 1 or 5 ml of supplemented TSB. Plates were incubated at 37°C for 24 h without shaking. Each day, biofilms were carefully washed once with 1 or 5 ml sterile PBS to wash away non-adherent cells, and fresh medium was added. This process was continued for a total of 3 to 5 days. To quantify biofilm formation, crystal violet stain was eluted from the biofilms with 100% ethanol and diluted 3-fold prior to reading the absorbance at 595 nm on a plate reading spectrophotometer (Molecular Devices OptiMAX microplate reader).

Long-term static biofilms on coverslips were made as described (23). Coverslips were collected on the final day, and the biofilms were washed and stained with BacLight kit dyes SYTO-9 (1.3 μM) and propidium iodide (PI; 4 μM). The coverslips were then flipped onto glass slides and sealed with nail polish.

A Zeiss 510-Meta confocal laser scanning microscope with a 63× oil immersion Plan-Apochromat objective was used to visualize the biofilms. A 488-nm argon laser was used for excitation of SYTO-9 with the emission band-pass filter set at a wavelength of 515 ± 15 nm. For excitation of PI, a 543-nm HeNe laser was used, and band-pass filters for emission were set at 630 ± 15 nm. Images were analyzed using Zeiss Image Examiner and ImageJ software. All image collection was done at the WM Keck Center for Advanced Studies in Neural Signaling (University of Washington).

**Statistical analysis.** Statistical analysis of results used Prism (GraphPad Software, La Jolla, CA). All Student's *t* tests were unpaired with a two-tailed 95% confidence interval. NO· consumption over time was analyzed using a matched 2-way analysis of variance (ANOVA) with Bonferroni post-tests comparing each mutant strain to the WT over time.

**Microarray data accession numbers.** Microarray data have been deposited into the GEO database under the manuscript title.

## SUPPLEMENTAL MATERIAL

Supplemental material for this article may be found at <http://mbio.asm.org/lookup/suppl/doi:10.1128/mBio.00696-13/-/DCSupplemental>.

- Figure S1, PDF file, 0.1 MB.
- Figure S2, PDF file, 0.1 MB.
- Figure S3, PDF file, 3.3 MB.
- Table S1, PDF file, 0.1 MB.
- Table S2, PDF file, 0.1 MB.

## ACKNOWLEDGMENTS

This work is supported by NIH grant AI39557 to F.C.F. and AI073780 to P.M.D.

We thank Kevin McIver and Mark Smeltzer for the gifts of plasmids and strains.

## REFERENCES

1. Kluytmans J, van Belkum A, Verbrugh H. 1997. Nasal carriage of *Staphylococcus aureus*: epidemiology, underlying mechanisms, and associated risks. *Clin. Microbiol. Rev.* 10:505–520.
2. Djupesland PG, Chatkin JM, Qian W, Haight JS. 2001. Nitric oxide in the nasal airway: a new dimension in otorhinolaryngology. *Am. J. Otolaryngol.* 22:19–32.
3. Fang FC. 2004. Antimicrobial reactive oxygen and nitrogen species: concepts and controversies. *Nat. Rev. Microbiol.* 2:820–832.
4. Richardson AR, Dunman PM, Fang FC. 2006. The nitrosative stress response of *Staphylococcus aureus* is required for resistance to innate immunity. *Mol. Microbiol.* 61:927–939.
5. Bang IS, Liu L, Vazquez-Torres A, Crouch ML, Stamler JS, Fang FC. 2006. Maintenance of nitric oxide and redox homeostasis by the *Salmonella* flavohemoglobin hmp. *J. Biol. Chem.* 281:28039–28047.
6. Rodionov DA, Dubchak IL, Arkin AP, Alm EJ, Gelfand MS. 2005. Dissimilatory metabolism of nitrogen oxides in bacteria: comparative reconstruction of transcriptional networks. *PLOS Comput. Biol.* 1:e55. doi:10.1371/journal.pcbi.0010055.
7. Tucker NP, Hicks MG, Clarke TA, Crack JC, Chandra G, Le Brun NE, Dixon R, Hutchings MI. 2008. The transcriptional repressor protein NsrR senses nitric oxide directly via a [2Fe-2S] cluster. *PLoS One* 3:e3623. doi:10.1371/journal.pone.0003623.
8. Gill SR, Fouts DE, Archer GL, Mongodin EF, Deboy RT, Ravel J, Paulsen IT, Kolonay JF, Brinkac L, Beanan M, Dodson RJ, Daugherty SC, Madupu R, Angiuoli SV, Durkin AS, Haft DH, Vamathevan J, Khouri H, Utterback T, Lee C, Dimitrov G, Jiang L, Qin H, Weidman J, Tran K, Kang K, Hance IR, Nelson KE, Fraser CM. 2005. Insights on evolution of virulence and resistance from the complete genome analysis of an early methicillin-resistant *Staphylococcus aureus* strain and a biofilm-producing methicillin-resistant *Staphylococcus epidermidis* strain. *J. Bacteriol.* 187:2426–2438.
9. Nakano MM, Geng H, Nakano S, Kobayashi K. 2006. The nitric oxide-responsive regulator NsrR controls ResDE-dependent gene expression. *J. Bacteriol.* 188:5878–5887.
10. Pragman AA, Yarwood JM, Tripp TJ, Schlievert PM, Pragman AA, Yarwood JM, Tripp TJ, Schlievert PM. 2004. Characterization of virulence factor regulation by SrrAB, a two-component system in *Staphylococcus aureus*. *J. Bacteriol.* 186:2430–2438.
11. Ulrich M, Bastian M, Cramton SE, Ziegler K, Pragman A, Bragonzi A, Memmi G, Wolz C, Schlievert PM, Cheung A, Döring G. 2007. The staphylococcal respiratory response regulator SrrAB induces *ica* gene transcription and polysaccharide intercellular adhesin expression, protecting *Staphylococcus aureus* from neutrophil killing under anaerobic growth conditions. *Mol. Microbiol.* 65:1276–1287.
12. Nakano MM. 2002. Induction of ResDE-dependent gene expression in *Bacillus subtilis* in response to nitric oxide and nitrosative stress. *J. Bacteriol.* 184:1783–1787.
13. Beenken KE, Blevins JS, Smeltzer MS. 2003. Mutation of *sarA* in *Staphylococcus aureus* limits biofilm formation. *Infect. Immun.* 71:4206–4211.
14. Richardson AR, Libby SJ, Fang FC. 2008. A nitric oxide-inducible lactate dehydrogenase enables *Staphylococcus aureus* to resist innate immunity. *Science* 319:1672–1676.
15. Throup JP, Zappacosta F, Lunsford RD, Annan RS, Carr SA, Lonsdale JT, Bryant AP, McDevitt D, Rosenberg M, Burnham MK. 2001. The *srhSR* gene pair from *Staphylococcus aureus*: genomic and proteomic ap-

- proaches to the identification and characterization of gene function. *Biochemistry* 40:10392–10401.
16. Masalha M, Borovok I, Schreiber R, Aharonowitz Y, Cohen G. 2001. Analysis of transcription of the *Staphylococcus aureus* aerobic class Ib and anaerobic class III ribonucleotide reductase genes in response to oxygen. *J. Bacteriol.* 183:7260–7272.
  17. Overton TW, Justino MC, Li Y, Baptista JM, Melo AM, Cole JA, Saraiva LM. 2008. Widespread distribution in pathogenic bacteria of di-iron proteins that repair oxidative and nitrosative damage to iron-sulfur centers. *J. Bacteriol.* 190:2004–2013.
  18. Waheed SM, Ghosh A, Chakravarti R, Biswas A, Haque MM, Panda K, Stuehr DJ. 2010. Nitric oxide blocks cellular heme insertion into a broad range of heme proteins. *Free Radic. Biol. Med.* 48:1548–1558.
  19. Voggu L, Schlag S, Biswas R, Rosenstein R, Rausch C, Götz F. 2006. Microevolution of cytochrome *bd* oxidase in staphylococci and its implication in resistance to respiratory toxins released by *Pseudomonas*. *J. Bacteriol.* 188:8079–8086.
  20. Gillaspay AF, Hickmon SG, Skinner RA, Thomas JR, Nelson CL, Smeltzer MS. 1995. Role of the accessory gene regulator (*agr*) in pathogenesis of staphylococcal osteomyelitis. *Infect. Immun.* 63:3373–3380.
  21. Beenken KE, Dunman PM, McAleese F, Macapagal D, Murphy E, Projan SJ, Blevins JS, Smeltzer MS. 2004. Global gene expression in *Staphylococcus aureus* biofilms. *J. Bacteriol.* 186:4665–4684.
  22. Blevins JS, Elasmri MO, Allmendinger SD, Beenken KE, Skinner RA, Thomas JR, Smeltzer MS. 2003. Role of *sarA* in the pathogenesis of *Staphylococcus aureus* musculoskeletal infection. *Infect. Immun.* 71:516–523.
  23. Hancock LE, Perego M. 2004. The *Enterococcus faecalis* *fsr* two-component system controls biofilm development through production of gelatinase. *J. Bacteriol.* 186:5629–5639.
  24. Gotz FBT, Schleifer K-H. 2006. The genera *Staphylococcus* and *Micrococcus*, p 5–75. In Dworkin M, Falkow S, Rosenberg E, Schleifer K-H, Stackebrandt E (ed), *Bacteria: firmicutes, cyanobacteria*. Springer Verlag, New York, NY.
  25. Hammer ND, Reniere ML, Cassat JE, Zhang Y, Hirsch AO, Indriati HM, Skaar EP. 2013. Two heme-dependent terminal oxidases power *Staphylococcus aureus* organ-specific colonization of the vertebrate host. *mBio* 4(4):e00241-13. doi:10.1128/mBio.00241-13.
  26. Taber HW, Morrison M. 1964. Electron transport in staphylococci. Properties of a particle preparation from exponential phase *Staphylococcus aureus*. *Arch. Biochem. Biophys.* 105:367–379.
  27. Forte E, Borisov VB, Konstantinov AA, Brunori M, Giuffrè A, Sarti P. 2007. Cytochrome *bd*, a key oxidase in bacterial survival and tolerance to nitrosative stress. *Ital. J. Biochem.* 56:265–269.
  28. Kohler C, von Eiff C, Liebeke M, McNamara PJ, Lalk M, Proctor RA, Hecker M, Engelmann S. 2008. A defect in menadiene biosynthesis induces global changes in gene expression in *Staphylococcus aureus*. *J. Bacteriol.* 190:6351–6364.
  29. Georgellis D, Kwon O, Lin EC. 2001. Quinones as the redox signal for the *arc* two-component system of bacteria. *Science* 292:2314–2316.
  30. Pagels M, Fuchs S, Pané-Farré J, Kohler C, Menschner L, Hecker M, McNamara PJ, Bauer MC, von Wachenfeldt C, Liebeke M, Lalk M, Sander G, von Eiff C, Proctor RA, Engelmann S. 2010. Redox sensing by a Rex-family repressor is involved in the regulation of anaerobic gene expression in *Staphylococcus aureus*. *Mol. Microbiol.* 76:1142–1161.
  31. Quoc TPH, Genevaux P, Pajunen M, Savilahti H, Georgopoulos C, Schrenzel J, Kelley WL. 2007. Isolation and characterization of biofilm formation-defective mutants of *Staphylococcus aureus*. *Infect. Immun.* 75:1079–1088.
  32. Pattee PA, Neveln DS. 1975. Transformation analysis of three linkage groups in *Staphylococcus aureus*. *J. Bacteriol.* 124:201–211.
  33. Roberts C, Anderson KL, Murphy E, Projan SJ, Mounts W, Hurlburt B, Smeltzer M, Overbeek R, Disz T, Dunman PM. 2006. Characterizing the effect of the *Staphylococcus aureus* virulence factor regulator, *SarA*, on log-phase mRNA half-lives. *J. Bacteriol.* 188:2593–2603.
  34. Brückner R. 1997. Gene replacement in *Staphylococcus carnosus* and *Staphylococcus xylosum*. *FEMS Microbiol. Lett.* 151:1–8.
  35. Novick RP. 1991. Genetic systems in staphylococci. *Methods Enzymol.* 204:587–636.